US and MRI in the evaluation of mammographic BI-RADS 4 and 5 microcalcifications

Hrkac Pustahija, Ana; Ivanac, Gordana; Brkljačić, Boris

Repository / Repozitorij:

Dr Med - University of Zagreb School of Medicine Digital Repository

US and MRI in the evaluation of mammographic BI-RADS 4 and 5 microcalcifications

Ana Hrkac Pustahija ⓘ
Gordana Ivanac ⓘ
Boris Brkljacic ⓘ

PURPOSE
The aim of this study was to assess diagnostic accuracies of ultrasonography (US) and magnetic resonance imaging (MRI) in lesions that manifest as mammographic BI-RADS 4 and 5 microcalcifications, in the setting of conjoined use of mammography, US, and MRI.

METHODS
Patients with mammographic BI-RADS 4 or 5 microcalcifications, without additional findings, were included in this prospective study. All patients subsequently underwent breast US and MRI. Histopathologic diagnosis, obtained by US-guided core-needle biopsy or surgical excision, served as a reference standard. Diagnostic accuracies of US and MRI were calculated, and positive predictive value for different MRI BI-RADS imaging features were determined.

RESULTS
The study group consisted of 113 women with 125 areas of suspicious microcalcifications. MRI reached sensitivity, specificity, positive predictive value 3 (PPV3), and negative predictive value (NPV) of 100%, 70.1%, 67.6%, and 100%, respectively. Statistically significant differences in MRI morphologic features and kinetic enhancement curves were observed between malignant and benign microcalcifications. Sensitivity, specificity, PPV3, and NPV for US were: 85.4%, 66.2%, 61.2%, and 87.9%. There was statistically significant difference in presentation of malignant and benign microcalcifications at US.

CONCLUSION
In the setting of conjoined use of mammography, US, and MRI, MRI can reliably exclude malignancy in suspicious microcalcifications. Thus, negative MRI findings may influence the decision to biopsy the microcalcifications.

Microcalcifications account for 31% of lesions detected at screening mammography, and are often considered to be an early sign of breast cancer (1, 2). Although easily detectable on mammography, they present a diagnostic challenge. Most mammographic microcalcifications are currently assessed by means of histopathologic workup of percutaneous biopsy specimens - histopathologic proof is still considered essential for the definitive diagnosis (3–5). However, low specificity of mammography leads to low positive predictive value (PPV) of biopsies based on mammographic referral (ranging from 21% to 42%) (6–9). These data indicate that a large proportion of biopsies yield benign results and, therefore, potentially could be avoided (8). Breast Imaging and Reporting System (BI-RADS) is aiming to help stratifying the risk of malignancy, but BI-RADS descriptors are often not consistently applied between the readers, and PPV of mammography remains low (6, 10, 11).

Other imaging methods do not have a universally accepted role in the detection and characterization of microcalcifications yet (3, 7). Ultrasonography (US), due to considerable variations of reported sensitivities, is not considered a reliable tool in the evaluation of microcalcifications (2, 5, 7, 12–14). Also, the role of magnetic resonance imaging (MRI) is still not firmly established. Guidelines of the European Society of Breast Imaging (EUSOBI) claim that the negative predictive value (NPV) of MRI (reported to be around 70%) is not sufficient to confidently downgrade lesions from suspicious to benign, and alter the decision about bi-

From the Department of Diagnostic and Interventional Radiology (B.B. ✉ boris@brkljacic. com), University Hospital Dubrava, University of Zagreb, School of Medicine, Zagreb, Croatia.

opsy (3, 4). Since 1996, several studies have investigated the diagnostic performance of MRI in classification of lesions that appear as mammographic microcalcifications, and reported results vary substantially (15).

Approximately 75% of ductal carcinoma in situ (DCIS) present with pure mammographic microcalcifications (16). DCIS is a disease process that is not well understood, in part because of its heterogeneous nature. Many studies aimed to assess prognostic factors to characterize its risk of invasive potential; however, there still remains a lack of agreement about its natural history, workup, and treatment (17–19). While there is lack of understanding of DCIS and its natural progression, improvements in identification of imaging findings related to DCIS may be useful. The most common mammography appearance for both high-grade and non–high-grade DCIS is fine pleomorphic calcifications, in segmental or linear distribution, as reflection of cell necrosis and dystrophic calcifications in the lumen of the terminal duct (20–23). US fea-

tures of DCIS include ductal abnormalities, architectural distortions, and in more than 70% of DCIS, hyperechoic foci can be detected on US; however, sonography is not the imaging modality of choice for diagnosis of DCIS (24). MRI is overall more sensitive than mammography in the detection of all grades of DCIS, with higher sensitivity for high-grade and intermediate-grade DCIS compared with low-grade DCIS (98%, 91%, and 80%, respectively) (20, 25–28). Most common MRI presentation of DCIS is non-mass lesions, with segmental distribution and clumped internal enhancement (29). MRI features of DCIS are related to specific growth pattern within the ducts and typical neovascularization: tumor cells can directly release angiogenic factors resulting in a rim of microvessels adjacent to the basement membrane of affected ducts or indirectly via recruitment of accessory cells leading to diffuse stromal vascularity (30). Additionally, slow enhancement of the actual DCIS ducts can also be due to gadolinium entering the leaky ducts (30, 31). However, MRI features of DCIS overlap with some benign lesions, such as fibrocystic changes, pseudoangiomatous stromal hyperplasia, and mastitis, which all can cause false-positive MRI findings (30, 32).

The aim of this study was to assess diagnostic accuracies of US and MRI in the characterization of lesions that manifest as mammographic BI-RADS 4 and 5 microcalcifications, in the setting of conjoined use of mammography, US, and MRI.

Methods

Study population

Eligible for this prospective study were women presenting with mammographic BI-RADS 4 and 5 microcalcifications, without associated mammographic findings. In further management, patients underwent breast US, followed by breast MRI. The histopathologic diagnosis, obtained by US-guided core-needle biopsy (CNB) or surgical excision, was set as reference standard. High-risk lesions obtained by CNB were confirmed by means of surgical excision. The results of CNB and surgical excision were followed by 1-year follow-up with mammography, US and MRI. The study design and protocol were reviewed and approved by the institutional review board. All patients signed informed consent after the nature of the study had been fully explained to them.

In a period of three years 164 women were enrolled in the study. In the final data analysis, 51 women were excluded for the following reasons: 15 because mammograms were incomplete (only hard copies of film-screen mammograms from outside facilities were available to the readers, with MLO and CC projections, without spot compression views), 6 patients did not undergo US, 4 did not undergo MRI (2 refused because of claustrophobia, 2 had technical contraindications – 1 pacemaker, 1 ferromagnetic metal foreign bodies), 10 had no histopathologic diagnosis (did not complete workup in our institution), and 16 cases were lost from follow-up. The final study group consisted of 113 patients with 125 areas of suspicious microcalcifications (age range 36–71 years, median 55 years).

Imaging methods

Mammograms included in the study had to be performed using a full field digital mammography system (76 were performed in our department, using Mammomat Novation DR Siemens). Standard mediolateral oblique and craniocaudal projections, with additional magnification views were performed. In 37 cases where no magnification views were available, electronic magnification (zooming) of digital mammograms was used at the viewing workstation.

US of the breasts was performed using high frequency linear-array broadband transducers with a frequency of 9–14 MHz and 9–15 MHz (Logiq 9, General Electric Healthcare, and Supersonic, Aixplorer® ultrasound system, SuperSonic Imagine). US examination was directed based on the mammographic estimation of the location of microcalcifications. US findings of the presumed area of mammographic microcalcifications were divided into groups of 1) visible changes, and 2) invisible changes. Visible changes were further subdivided into: a) microcalcifications (observed as hyperechoic dots) within hypoechoic area/mass or dilated ducts, b) isolated microcalcifications, without associated findings, c) other parenchymal changes (heterogeneous areas without significant hypoechoic area/mass or clearly visible microcalcifications).

Breast MRI was performed at 1.5 T (Magnetom Avanto, Siemens). A dedicated breast coil was used, with the imaging protocol consisting of following sequences: axial T2-weighted TIRM (TI: 150.0 ms, TR: 4330.0 ms, TE: 69.0 ms, slice thickness 4

Main points

- When mammography, US, and MRI are used in conjunction for the workup of BI-RADS 4 and 5 microcalcifications, MRI reaches 100% sensitivity, 70.1% specificity, 67.6% positive predictive value (PPV3), and 100% negative predictive value (NPV). This means that negative MRI finding in such clinical setting may confidently rule out malignancy, and thus, influence the decision to perform biopsy of microcalcifications.

- When MRI BI-RADS descriptors are applied in analysis, microcalcifications present most commonly as non-mass lesions, with statistically significant difference in presentation of malignant and benign microcalcifications. Highest risk of malignancy is found for segmental distribution and clumped internal enhancement.

- US has shown clinically unacceptable values for test performance as a method for ruling out malignancy, with 100% sensitivity, 66.2% specificity, 61.2% PPV3, and 87.9% NPV.

- In cases when microcalcifications are visualized with US (78.4% of cases in our study), there is statistically different presentation between malignant and benign microcalcifications. Thus, recognizing specific patterns of US presentation of malignant and benign microcalcifications may add additional value to the MRI performance. US finding of "hyperechoic dots within hypoechoic mass, area or dilated ducts" is most commonly related to malignancy, while finding of "isolated microcalcifications within normal breast tissue" is seen only in benign cases.

mm, 320 mm field of view [FoV]), sagittal T2-weighted fast spin echo with fat saturation (TR: 7300.0 ms, TE: 113.0 ms, slice thickness 4 mm, 180 mm FoV), axial T2-weighted turbo spin echo (TR: 4000.0 ms, TE: 60.0 ms, slice thickness 4 mm, 380 mm FoV), axial T1-weighted three-dimensional (3D) gradient echo with fat saturation (TR: 4.3 ms, TE: 1.3 ms, slice thickness 0.8 mm, 340 mm FoV). Axial T1-weighted 3D gradient echo without fat saturation (TR: 16.0 ms, TE: 4.8 ms, slice thickness 2 mm, 320 mm FoV) before contrast administration and dynamic 3D axial T1-weighted gradient echo without fat saturation five times after the injection of the bolus of 0.1 mmol/kg of paramagnetic contrast agent (gadoterate meglumine, Dotarem ®) for both breasts were collected. Unenhanced images were then subtracted from the contrast- enhanced images on a pixel-by-pixel basis. Multiplanar reformatting (MPR) reconstructions and maximum intensity projection (MIP) reconstructions were performed, with dynamic (kinetic) time-intensity curves generated in the selected region of interest (ROI).

CNB was performed after MRI, under US guidance, using a 14-gauge biopsy device (Monopty, Bard), with multiple passes per lesion. Mammography of the specimen was performed in order to confirm the presence of microcalcifications in the specimen. In patients with surgical excision of lesions, wire localization of microcalcifications was performed under US and correct position was confirmed by mammography. For sonographically invisible lesions, mammography guidance of biopsy, with a fenestrated compression paddle with alpha-numeric grid, was used.

Statistical analysis

Imaging findings were analyzed and reported using BI-RADS descriptors (10, 11). To calculate diagnostic accuracies of imaging methods, findings were dichotomized: negative examinations were defined as examinations with BI-RADS final assessment category of 1–3, while positive examinations were defined as examinations with final assessment category of 4 and 5. Positive predictive value (PPV) was calculated as the number of detected cancers per positive examinations. The positive predictive value category 3 (PPV3) defined as per BI-RADS Atlas 5th edition is the rate of detected cancers (true positive) divided by all patients in whom biopsy was performed (true positive and false positive) (11). Since all our patients had biopsy performed af-

ter imaging work-up was finished, PPV3 was calculated in all cases. Sensitivity was calculated as the number of positive examinations for which there was a tissue diagnosis of cancer, divided by all cancers present in the study group. Specificity was calculated as the number of negative examinations for which there was no tissue diagnosis of cancer, divided by all examinations for which there was no tissue diagnosis of cancer. Negative predictive value (NPV) was calculated as the number of negative examinations for which there was no tissue diagnosis of cancer, divided by all negative examinations.

All clinical and imaging data were available to the reading radiologist, and findings were presented and discussed at the multidisciplinary breast team meetings. Mammographic and MRI examinations were interpreted by one of three co-authors (radiologists with 10–22 years of experience in breast imaging). Screening mammograms were evaluated by two radiologists independently and diagnostic mammograms by one. US exams and CNB were performed by a single examiner with 22 years of experience in breast imaging.

Data were analyzed using the Statistical Package for Social Sciences 16.0 (SPSS Inc.). Chi square, Fisher's exact test and the Mann-Whitney U test were used for comparison of the groups, with two-tailed P value less than 0.05 considered statistically significant. Study sample size requirements were calculated based on a clinically acceptable degree of precision, at the estimated prevalence of disease in the target population, and at the hypothesized values of sensitivity, specificity, and predictive values; thus, at the estimated prevalence of the disease in the target population of 40% and at the hypothesized value of sensitivity equal to 85% the calculated required sample size was 123, and at the hypothesized value of specificity equal to 75% the calculated required sample size was 120, based on a 95% confidence interval of hypothesized sensitivity and specificity (33).

Results

Histologic diagnoses are presented in Table 1. Prevalence of malignancy in our study group was 38.4% (48/125). As shown in Table 1, pure DCIS comprised 52.1% of malignant cases, microinvasive lesions further 12.5%, and invasive lesions 35.4%. The details of other histopathologic findings can be found in Table 1.

Table 1. Histopathologic diagnoses of mammographic BI-RADS 4 and 5 microcalcifications in our study

Histologic diagnosis	No. of cases (%)
Malignant (n=48, 38.4%)	
DCIS	25 (52.1)
IDC	21 (43.8)
IDC+DCIS	7
DC mic	6
IDC	8
ILC	2 (4.2)
Total	48 (100)
Benign (n=77, 61.6%)	
Sclerosing adenosis	16 (20.8)
Flat epithelial atypia	6 (7.8)
Complex sclerosing adenosis	4 (5.2)
LCIS	4 (5.2)
ADH	2 (2.6)
Intraductal papilloma	2 (2.6)
Other benign changes- B2	43 (55.8)
Total	77 (100)

DCIS, ductal carcinoma in situ; IDC, invasive ductal carcinoma; DC mic, microinvasive ductal carcinoma; ILC, invasive lobular carcinoma; LCIS, lobular carcinoma in situ; ADH, atypical ductal hyperplasia.

Table 2. Correlation of sonographic visibility of microcalcifications with histologic findings, mammographic diameter and mammographic BI-RADS category

	US visible, n (%)	US invisible, n (%)	P
Histologic findings			0.18
Malignant disease	41 (85.4)	7 (14.6)	
Benign disease	57 (74.0)	20 (26.0)	
Total	98 (78.4)	27 (21.6)	
Mammographic size of cluster (mm), median (range)	29 (5–85)	20 (6–58)	0.037
Mammographic BI-RADS category			0.20
BI-RADS 4	89 (76.7)	27 (23.3)	
BI-RADS 5	9 (100)	0 (0)	

BI-RADS, breast imaging-reporting and data system.

Table 3. US features of mammographic BI-RADS 4 and 5 microcalcifications

	Malignant	Benign	Total (%)	PPV3
US findings*				
Microcalcifications within hypoechoic mass, area or dilated ducts	35	17	52 (41.6)	67.3%
Isolated microcalcifications	0	9	9 (7.2)	0
Heterogeneous regions without mass or clearly visible microcalcifications	6	31	37 (29.6)	16.2%
Negative (US invisible microcalcifications)	7	20	27 (21.6)	25.9%
Total	48	77	125 (100)	
US BI-RADS 1–3	7	51	58 (46.4)	
US BI-RADS 4–5	41	26	67 (53.6)	

BI-RADS, breast imaging-reporting and data system; US, ultrasonography; PPV3, positive predictive value calculated based on performed biopsy.
*US findings of microcalcifications were significantly different between benign and malignant cases ($P < 0.001$).
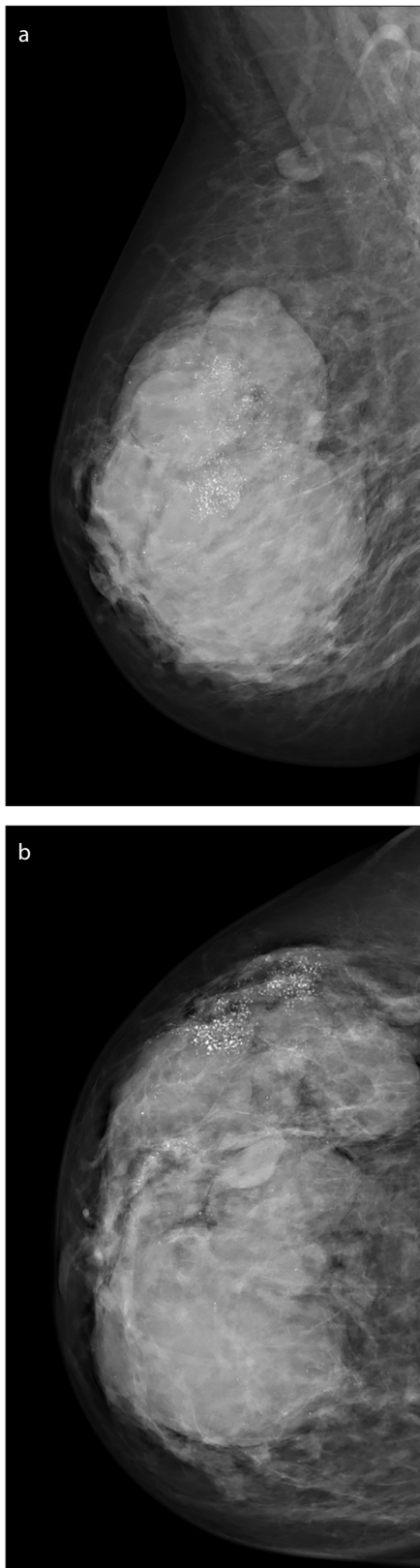
Figure 1. a, b. Mammography, mediolateral oblique (**a**) and craniocaudal (**b**) projections: fine pleomorphic and linear branching microcalcifications, in segmental distribution, in the upper outer quadrant of the right breast. Multiple lobulated densities are seen in all quadrants.

Mammography as indicator for biopsy yielded PPV3 of 38.4%. Separately, mammographic BI-RADS 4 category yielded PPV3 of 34.5% (40/116 malignant microcalcifications), and BI-RADS 5 had PPV3 of 88.9% (8/9 malignant).

Results of US in workup of microcalcifications are shown in Tables 2 and 3. Sensitivity, specificity, PPV3, and NPV for US were: 85.4% (95% CI, 72.2– 93.9), 66.2% (95% CI, 54.5– 76.6), 61.2% (95% CI, 48.5–72.8), and 87.9% (95% CI, 76.7– 95.0). Overall, changes associated with microcalcifications were seen on US in 78.4% of cases. Malignant microcalcifications were more likely to be visible on US (85.4% of cases) compared to benign ones (74%). However, difference in visibility between malignant and benign lesions did not reach statistical significance ($P = 0.18$). As summarized in Table 3, malignant and benign microcalcifications presented differently on US, with statistically significant difference. Finding "hyperechoic dots within hypoechoic mass, area or dilated ducts" was most commonly related to malignancy, with the highest PPV3 (67.3%). Isolated microcalcifications within normal breast tissue were seen only in benign cases, with NPV of 100%. High-risk lesions comprised a higher portion of false positive findings (44.4%, 8/18). Among false negative findings of US, 71.4% (5/7) were pure DCIS lesions, while the rest (28.6%, 2/7) were invasive lobular carcinoma.

Microcalcifications visible on US had larger mammographic diameter compared with those invisible on US, with statistically significant difference (median of mam-

Table 4. MRI features of pure microcalcifications in correlation to histopathology

	Malignant	Benign	Total (%)	PPV3	P
MRI BI-RADS category					
MRI BI-RADS 1	0	0	0 (0)	0	
MRI BI-RADS 2	0	21	21 (16.8)	0	
MRI BI-RADS 3	0	33	33 (26.4)	0	
MRI BI-RADS 4	8	21	29 (23.2)	27.6%	
MRI BI-RADS 5	40	2	42 (33.6)	95.2%	
Total	48	77	125 (100)		
Morphology					<0.001
Mass	16	8	24 (19.2)	66.7%	
Non-mass enhancement	32	41	73 (58.4)	43.8%	
Focus	0	28	28 (22.4)	0	
Total	48	77	125 (100)		
Kinetic curve type					<0.001
Wash-out	29	8	37 (38.1)	78.4%	
Plateau	17	17	34 (35.1)	50.0%	
Persistent	2	24	26 (26.8)	7.7%	
Total	48	49	97 (100)		
Mass shape					0.16
Round	3	2	5 (20.8)	60.0%	
Oval	3	3	6 (25)	50.0%	
Lobulated	1	2	3 (12.5)	33.3%	
Irregular	9	1	10 (41.7)	90.0%	
Total	16	8	24 (100)		
Mass margin					0.007
Smooth	0	4	4 (16.7)	0	
Irregular	12	4	16 (66.7)	75.0%	
Spiculated	4	0	4 (16.7)	100.0%	
Total	16	8	24 (100)		
Mass enhancement					<0.001
Homogeneous	0	4	4 (16.7)	0	
Heterogeneous	16	2	18 (75.0)	88.9%	
Dark internal septa	0	2	2 (8.3)	0	
Enhancing internal septa	0	0	0 (0)	0	
Rim	0	0	0 (0)	0	
Central	0	0	0 (0)	0	
Total	16	8	24 (100)		
Non-mass distribution					<0.001
Focal	0	19	19 (26)	0	
Linear	1	3	4 (5.5)	25.0%	
Ductal	2	2	4 (5.5)	50.0%	
Segmental	19	9	28 (38.4)	67.9%	
Regional	10	8	18 (24.7)	55.6%	

mographic diameters: 29 mm vs. 20 mm; P = 0.037) (Table 2).

Detailed MRI features of microcalcifications are presented in Table 4. Sensitivity, specificity, PPV3, and NPV of MRI were 100% (95% CI, 92.6–100), 70.1% (95% CI, 58.6–80.0), 67.6% (95% CI, 55.5–78.2), and 100% (95% CI, 93.4–100). Overall, non-mass lesion enhancement was the most common presentation of microcalcifications (58.4% of all cases). We compared diagnostic accuracies separately for masses and non-mass lesions to test the influence of lesion type on diagnostic capabilities of MRI. There was no statistically significant association between lesion type and diagnostic accuracy (P = 0.59): sensitivity, specificity, PPV3, and NPV for masses were 100% (95% CI, 79.4–100), 50% (95% CI, 15.7–84.3), 80% (95% CI, 56.3–94.3), and 100% (95% CI, 39.8–100), and for non-mass lesions 100% (95% CI, 89.1–100), 53.7% (95% CI, 37.4–69.4), 62.6% (95% CI, 48.0–75.9), and 100% (95% CI, 84.6–100). However, masses had higher probability to be malignant (PPV3, 66.7%), compared with non-mass lesions (PPV3, 43.8%).

Figs. 1–3 show representative cases of conjoined mammography, US, and MRI workup of microcalcifications. Histologic diagnosis after second-look US-guided CNB was atypical ductal hyperplasia. Wide surgical excision was recommended because of highly suspicious findings of MRI. Diagnosis after excision was multiple foci of DCIS, and because of widespread area of non-mass enhancement seen on MRI, mastectomy was performed. Final diagnosis was microinvasive ductal carcinoma.

Discussion

In this study, consecutive enrollment of mammography, US, and MRI in the workup of microcalcifications resulted in MRI sensitivity of 100%, with NPV of 100%. Although estimated PPV3 for the MRI was only moderate (67.6%), it is still a significant improvement compared with PPV3 of mammography alone (which was 38.4% in our study, and according to literature ranges from 21% to 42%) (6–9). Such conjoined approach, with US and MRI used in addition to mammography in workup of microcalcifications, has not been so far published in the literature (3, 4, 31, 34–43).

Concerning the role of US in the assessment of microcalcifications, in our study 78.4% of microcalcifications were identified at US. Those rates are very heterogeneous

Table 4. MRI features of pure microcalcifications in correlation to histopathology (cont'd)

Multiple regions	0	0	0 (0)	0	
Diffuse	0	0	0 (0)	0	
Total	32	41	73 (100)		
Non-mass internal enhancement					<0.001
Homogeneous	0	1	1 (1.4)	0	
Heterogeneous	0	14	14 (19.2)	0	
Stippled	2	16	18 (24.7)	11.1%	
Clumped	30	10	40 (54.8)	75.0%	
Reticular	0	0	0 (0)	0	
Total	32	41	73 (100)		

MRI, magnetic resonance imaging; BI-RADS, breast imaging-reporting and data system; PPV3, positive predictive value calculated based on performed biopsy.
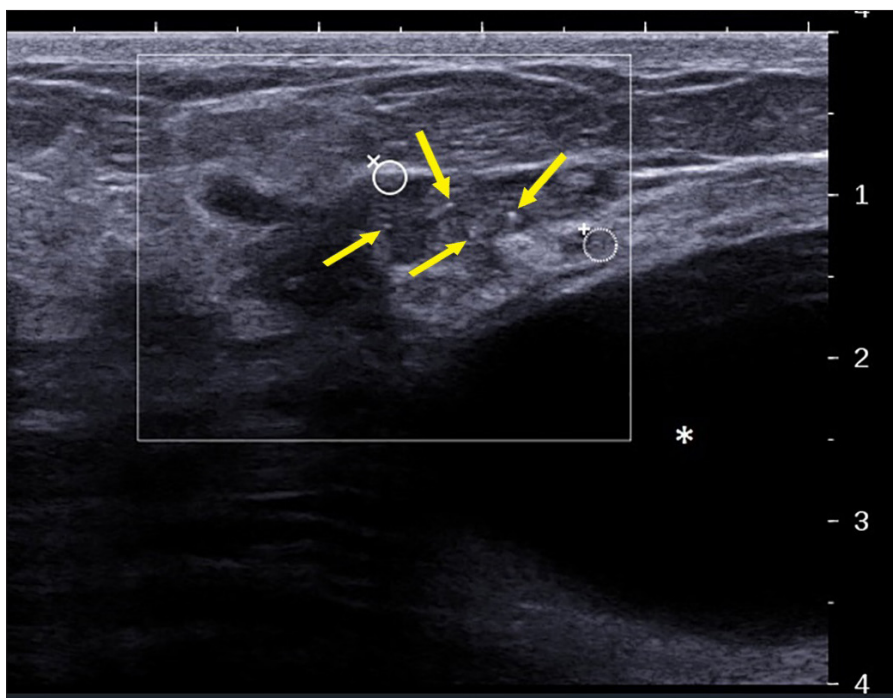

Figure 2. Ultrasound: microcalcifications were in B-mode visible as hyperechoic dots *(yellow arrows)* surrounded by heterogeneous irregular area. Multiple large cysts in all quadrants *(asterisk)* correlated with lobulated densities visible on mammography. Circles with "x" and "+" marks remained from elastography measurements, which were not analyzed in this study.

far published in the literature. To our knowledge, there are only two previous studies which analyzed individual MRI BI-RADS descriptors associated with malignancy in cases of microcalcifications, and our results are in agreement with earlier published data (31, 41). However, no prior study assessed PPVs of different MRI features in the workup of microcalcifications. As shown in Table 4, MRI morphologic features of masses with highest PPV3 in our study were irregular shape, spiculated margin, and heterogeneous internal enhancement. For the non-mass enhancement lesions, malignancy was typically represented by segmental distribution and clumped internal enhancement. Wash-out kinetic dynamic enhancement curve was highly indicative of malignancy, both for masses and non-mass lesions.

We analyzed earlier reports on diagnostic performances of MRI in workup of microcalcifications (3, 4, 31, 34–43). Those reports vary substantially in methodology and results, with sensitivities ranging from 45% to 100%, and specificities from 51% to 100%. Recently, a review and meta-analysis study was published by Bennani-Baiti and Baltzer (15), aiming to clarify the role of MRI in assessment of mammographic BI-RADS 3–5 microcalcifications. Twenty studies met their inclusion criteria, with 1843 lesions and a mean prevalence of malignancy of 40.6%. It is interesting that seven of those 20 studies were published after 2014, while the oldest study dated from 1996. Authors revealed pooled sensitivity and specificity of 92% and 82% for BI-RADS 4 lesions, 95% and 66% for BI-RADS 5 lesions, and 57% and 32% for BI-RADS 3 lesions. Their conclusion was that MRI is not recommended for diagnosis of malignancy in BI-RADS 3 and 5 mammographic microcalcifications but can be considered for BI-RADS 4 microcalcifications.

We analyzed potential biases which might have influenced our results. As shown in our study, pure microcalcifications present most commonly as non-mass lesions (Table 4). Non-mass lesions are well recognized as the problem makers in breast MRI: most readers have problems in the interpretation of non-mass lesions, while inexperienced readers' ability to differentiate benign from malignant non-mass lesion can be close to guessing (6). This points out importance of experience in cases of microcalcifications. In our study only experienced readers were included, but we did not perform interob-
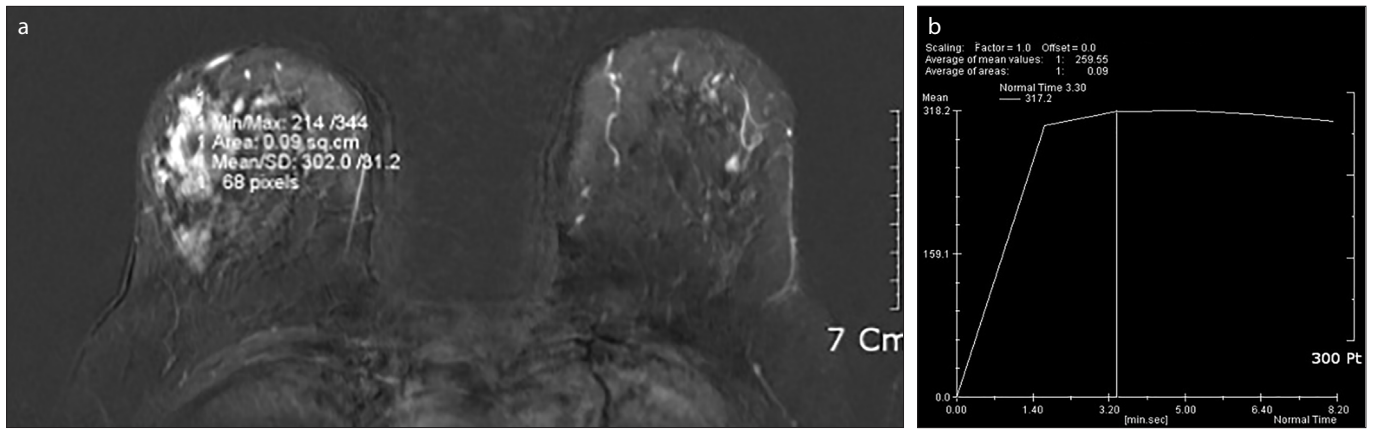
in the literature, and vary from 23% to 97% (2, 5, 7, 12, 44, 45). But, we have found that, when microcalcifications are visualized with US, there is a statistically different presentation between malignant and benign microcalcifications. US finding of "hyperechoic dots within hypoechoic mass, area or dilated ducts" was most commonly related to malignancy, while finding of "isolated microcalcifications within normal breast tissue" was seen only in benign cases. Also, malignant microcalcifications in our study were more commonly visualized than benign (85.4%

vs. 74%), which is in accordance with other studies (2, 14, 46). This permits us to presume that recognition of such different patterns of sonographic presentation of microcalcifications may add additional value when performing MRI after US, and thus improve MRI performance for microcalcifications.

Regarding different MRI BI-RADS imaging features, we noticed that lesion type (mass vs. non-mass) did not influence significantly on the diagnostic accuracy of MRI, with similar sensitivity and specificity for both subgroups, which is opposite to the findings so

Figure 3. a, b. Subtracted postcontrast MRI **(a)** shows non-mass lesion of the right breast, with clumped internal enhancement and regional distribution. Dynamic-kinetic curve with ROI inside non-mass lesion had rapid enhancement in initial phase with plateau in the delayed phase **(b)**. Second-look US-guided core needle biopsy revealed atypical ductal hyperplasia. Suspicious imaging findings indicated open surgical excision. Upon mastectomy microinvasive ductal carcinoma was proven.

server variability analysis, which prevents us from drawing a conclusion about the influence of readers' experience on results. Next potential bias is patient selection procedure. There are some reports that performances of MRI in microcalcifications are somewhat better for invasive lesions (15). Prevalence of malignancy in our study was 38.4%, which is close to average published rates (around 40%), and declines one of the possible patient selection biases. Prevalence of DCIS among malignant lesions is also recognized as a potential cause of lower specificity of MRI in microcalcifications. In the review study published by Bennani-Baiti and Baltzer (15), among 1843 lesions, there were 106 false-negative findings (5.8%), 68 of which (64.2%) were DCIS only. When DCIS was excluded, the pooled negative predictive value of breast MRI to rule out invasive or microinvasive cancer was found to be significantly higher, reaching 99%. DCIS comprised 52.1% of our malignant cases (Table 1) and was the major cause of false negative findings of US in our study (71.4%). But, as mentioned earlier, we did not have false negative MRI findings, so we cannot assess the influence of DCIS on sensitivity of MRI in our study.

There are several limitations to our study. First, vacuum-assisted biopsy is considered the method of choice in cases of pure microcalcifications. We used US-guided CNB due to organization of work in our facility but tried to address this issue by having a single highly experienced radiologist perform all US-guided CNB (22 years of experience in breast imaging, including US). Also, mammography of biopsy specimens was performed to confirm the presence of microcalcifications. Second, we did not perform interobserver variability tests for MRI results, which leaves us without quantitative analysis of the exact effect of experience on diagnostic accuracy of a method. Also, we did not perform blinded MRI reading (without knowledge of prior US findings). Therefore, we cannot compare blinded and non-blinded results, and thus cannot assess exact influence of performing US prior to MRI on final results of MRI. We can just assess combined methods diagnostic accuracy (US + MRI), presented through diagnostic accuracy achieved with MRI. We did not perform detailed analysis on different subgroups of cases (such as US or MRI features for different histologic diagnoses, for different type of microcalcifications according to mammographic BI-RADS descriptors, for breast density, patients, hereditary risk for breast carcinoma, correlation of microcalcifications area diameter to MRI findings), which prevents us from analyzing the influence of those covariates on our results. Finally, we did not analyze the number of false positive findings found on MRI in the contralateral breast or in other parts of the same breast.

In conclusion, the aim of our study was to test the suitability of conjoined use of mammography, US, and MRI in the evaluation of mammographic BI-RADS 4 and 5 microcalcifications. In such settings, MRI reaches NPV of 100%, which supports the application of MRI for exclusion of malignancy, and suggests that negative MRI may influence the decision to biopsy microcalcifications. However, further work with larger number of cases is needed to validate our results. There is statistically significant difference in presentation between malig-

nant and benign microcalcifications when MRI BI-RADS descriptors are applied in the analysis. Microcalcifications appear most commonly as non-mass lesions, which is important to keep in mind when MRI is used for the workup of microcalcifications, since non-mass lesions are the major cause of possible false negative findings of MRI. On the other hand, US cannot reliably exclude malignancy nor decline the need for biopsy. However, when microcalcifications are visualized with US prior to MRI, recognition of a different pattern of sonographic presentation of malignant and benign microcalcifications may add additional value to the performance of MRI.

Conflict of interest disclosure

The authors declared no conflicts of interest.

References

1. Naseem M, Murray J, Hilton JF, et al. Mammographic microcalcifications and breast cancer tumorigenesis: a radiologic-pathologic analysis. BMC Cancer 2015; 15:307. **[CrossRef]**
2. Kang SS, Ko EY, Han B-K, Shin JH. Breast US in patients who had microcalcifications with low concern of malignancy on screening mammography. Eur J Radiol 2008; 67:285–291. **[CrossRef]**
3. Mann RM, Kuhl CK, Kinkel K, Boetes C. Breast MRI: guidelines from the European Society of Breast Imaging. Eur Radiol 2008; 18:1307–1318. **[CrossRef]**
4. Bluemke DA, Gatsonis CA, Chen MH, et al. Magnetic resonance imaging of the breast prior to biopsy. JAMA 2004; 292:2735–2742. **[CrossRef]**
5. Cheung Y-C, Wan Y-L, Chen S-C, et al. Sonographic evaluation of mammographically detected microcalcifications without a mass prior to stereotactic core needle biopsy. J Clin Ultrasound 2002; 30:323–331. **[CrossRef]**

6. Bent CK, Bassett LW, D'Orsi CJ, Sayre JW. The positive predictive value of BI-RADS microcalcification descriptors and final assessment categories. AJR Am J Roentgenol 2010; 194:1378–1383. [CrossRef]

7. Moon WK, Im JG, Koh YH, Noh DY, Park IA. US of mammographically detected clustered microcalcifications. Radiology 2000; 217:849–854. [CrossRef]

8. Esen G, Tutar B, Uras C, Calay Z, İnce Ü, Tutar O. Vacuum-assisted stereotactic breast biopsy in the diagnosis and management of suspicious microcalcifications. Diagn Interv Radiol 2016; 22:326–333. [CrossRef]

9. Stehouwer BL, Merckel LG, Verkooijen HM, et al. 3-T breast magnetic resonance imaging in patients with suspicious microcalcifications on mammography. Eur Radiol 2014; 24:603–609. [CrossRef]

10. D'Orsi CJ, Mendelson, EB, Ikeda DM, et al. Breast Imaging Reporting and Data System: ACR BI-RADS – Breast Imaging Atlas, Reston, VA, American College of Radiology, 2003.

11. American College of Radiology, BI-RADS Committee. ACR BI-RADS atlas: breast imaging reporting and data system. Reston, VA: American College of Radiology; 2013.

12. Gufler H, Buitrago-Téllez CH, Madjar H, Allmann KH, Uhl M, Rohr-Reyes A. Ultrasound demonstration of mammographically detected microcalcifications. Acta Radiol 2000; 41:217–221. [CrossRef]

13. Cho N, Moon WK, Cha JH, et al. Ultrasound-guided vacuum-assisted biopsy of microcalcifications detected at screening mammography. Acta Radiol 2009; 50:602–609. [CrossRef]

14. Soo MS, Baker JA, Rosen EL. Sonographic detection and sonographically guided biopsy of breast microcalcifications. AJR Am J Roentgenol 2003; 180:941–948. [CrossRef]

15. Bennani-Baiti B, Baltzer PA. MR imaging for diagnosis of malignancy in mammographic microcalcifications: a systematic review and meta-analysis. Radiology. 2017; 283:692–701. [CrossRef]

16. Barreau B, de Mascarel I, Feuga C, et al. Mammography of ductal carcinoma in situ of the breast: review of 909 cases with radiographic-pathologic correlations. Eur J Radiol 2005; 54:55–61. [CrossRef]

17. Francis A, Thomas J, Fallowfield L, et al. Addressing overtreatment of screen detected DCIS; the LORIS trial. Eur J Cancer 2015; 51:2296–2303. [CrossRef]

18. Feinberg J, Wetstone R, Greenstein D, Borgen P. Is DCIS Overrated? Cancer Treat Res. 2018; 173:53–72. [CrossRef]

19. Parikh U, Chhor CM, Mercado CL. Ductal carcinoma in situ: the whole truth. AJR Am J Roentgenol 2018; 210:246–255. [CrossRef]

20. Greenwood HI, Heller SL, Kim S, Sigmund EE, Shaylor SD, Moy L. Ductal carcinoma in situ of the breasts: review of MR imaging features. Radiographics 2013; 33:1569–1588. [CrossRef]

21. Hofvind S, Iversen BF, Eriksen L, Styr BM, Kjellevold K, Kurz KD. Mammographic morphology and distribution of calcifications in ductal carcinoma in situ diagnosed in organized screening. Acta Radiol 2011; 52:481–487. [CrossRef]

22. Bluekens AMJ, Holland R, Karssemeijer N, Broeders MJM, den Heeten GJ. Comparison of digital screening mammography and screen-film mammography in the early detection of clinically relevant cancers: a multicenter study. Radiology 2012; 265:707–714. [CrossRef]

23. Evans A, Pinder S, Wilson R, et al. Ductal carcinoma in situ of the breast: correlation between mammographic and pathologic findings. AJR Am J Roentgenol 1994; 162:1307–1311. [CrossRef]

24. Brkljačić B, Ivanac G. Ultrasonography of the breast. Ultrasound Clinics 2014; 9:391–427. [CrossRef]

25. Kuhl CK, Schrading S, Bieling HB, et al. MRI for diagnosis of pure ductal carcinoma in situ: a prospective observational study. Lancet 2007; 370:485–492. [CrossRef]

26. Virnig BA, Tuttle TM, Shamliyan T, Kane RL. Ductal carcinoma in situ of the breast: a systematic review of incidence, treatment, and outcomes. J Natl Cancer Inst 2010; 102:170–178. [CrossRef]

27. Strobel K, Schrading S, Hansen NL, Barabasch A, Kuhl CK. Assessment of BI-RADS category 4 lesions detected with screening mammography and screening US: utility of MR imaging. Radiology 2015; 274:343–351. [CrossRef]

28. Menell JH, Morris EA, Dershaw DD, Abramson AF, Brogi E, Liberman L. Determination of the presence and extent of pure ductal carcinoma in situ by mammography and magnetic resonance imaging. Breast J 2005; 11:382–390. [CrossRef]

29. Rosen EL, Smith-Foley SA, DeMartini WB, Eby PR, Peacock S, Lehman CD. BI-RADS MRI enhancement characteristics of ductal carcinoma in situ. Breast J 2007; 13:545–550. [CrossRef]

30. Dietzel M, Kaiser CG, Wenkel E, et al. Differentiation of ductal carcinoma in situ versus fibrocystic changes by magnetic resonance imaging: are there pathognomonic imaging features? Acta Radiol 2017; 58:1206–1214. [CrossRef]

31. Kuhl CK. Why do purely intraductal cancers enhance on breast MR images? Radiology 2009; 253:281–283. [CrossRef]

32. Bowman E, Oprea G, Okoli J, et al. Pseudoangiomatous stromal hyperplasia (PASH) of the breast: a series of 24 patients. Breast J 2012; 18:242–247. [CrossRef]

33. Buderer NM. Statistical methodology: I. Incorporating the prevalence of disease into the sample size calculation for sensitivity and specificity. Acad Emerg Med 1996; 3:895–900. [CrossRef]

34. Strobel K, Schrading S, Hansen NL, Barabasch A, Kuhl CK. Assessment of BI-RADS category 4 lesions detected with screening mammography and screening US: utility of MR imaging. Radiology 2015; 274:343–351. [CrossRef]

35. Bazzocchi M, Zuiani C, Panizza P, et al. Contrast-enhanced breast MRI in patients with suspicious microcalcifications on mammography: results of a multicenter trial. AJR Am J Roentgenol 2006; 186:1723–1732. [CrossRef]

36. Akita A, Tanimoto A, Jinno H, Kameyama K, Kuribayashi S. The clinical value of bilateral breast MR imaging: is it worth performing on patients showing suspicious microcalcifications on mammography? Eur Radiol 2009; 19:2089–2096. [CrossRef]

37. Cilotti A, Iacconi C, Marini C, et al. Contrast-enhanced MR imaging in patients with BI-RADS 3-5 microcalcifications. Radiol Med 2007; 112:272–286. [CrossRef]

38. Kikuchi M, Tanino H, Kosaka Y, et al. Usefulness of MRI of microcalcification lesions to determine the indication for stereotactic mammotome biopsy. Anticancer Res 2014; 34:6749–6753.

39. Gilles R, Meunier M, Lucidarme O, et al. Clustered breast microcalcifications: evaluation by dynamic contrast-enhanced subtraction MRI. J Comput Assist Tomogr 1996; 20:9–14. [CrossRef]

40. Kneeshaw PJ, Lowry M, Manton D, Hubbard A, Drew PJ, Turnbull LW. Differentiation of benign from malignant breast disease associated with screening detected microcalcifications using dynamic contrast enhanced magnetic resonance imaging. Breast 2006; 15:29–38. [CrossRef]

41. Nakahara H, Namba K, Fukami A, et al. Three-dimensional MR imaging of mammographically detected suspicious microcalcifications. Breast Cancer 2001; 8:116–124. [CrossRef]

42. Yamamoto N, Yoshizako T, Yoshikawa K, Itakura M, Maruyama R, Kitagaki H. Breast 3 T-MR imaging: indication for stereotactic vacuum-assisted breast biopsy. Springerplus 2014; 3:481. [CrossRef]

43. Brnic D, Brnic D, Simundic I, Vanjaka Rogosic L, Tadic T. MRI and comparison mammography: a worthy diagnostic alliance for breast microcalcifications? Acta Radiol 2016; 57:413–421. [CrossRef]

44. Cho N, Moon WK, Cha JH, et al. Sonographically guided core biopsy of the breast: comparison of 14-gauge automated gun and 11-gauge directional vacuum-assisted biopsy methods. Korean J Radiol 2005; 6:102–9. [CrossRef]

45. Soo MS, Baker JA, Rosen EL, Vo TT. Sonographically guided biopsy of suspicious microcalcifications of the breast: a pilot study. AJR Am J Roentgenol 2002; 178:1007–1015. [CrossRef]

46. Bae S, Yoon JH, Moon HJ, Kim MJ, Kim E-K. Breast microcalcifications: diagnostic outcomes according to image-guided biopsy method. Korean J Radiol 2015; 16:996–1005. [CrossRef]